2012 International Conference on Fluid Dynamics and Thermodynamics Technologies (FDTT 2012)
IPCSIT vol.33(2012)©(2012) IACSIT Press, Singapore

Linear Biglobal Stability Analysis of Poiseuille-Rayleigh-Bénard Duct Flows in Binary Fluids with Soret Effect

Jun Hu[1], Daniel Henry[2], Xieyuan Yin[3] and Hamda BenHadid[2]

[1] Institute of Applied Physics and Computational Mathematics, Beijing 100088, China

[2] Laboratoire de Mécanique des Fluides et d'Acoustique, CNRS/Université de Lyon,

Ecole Centrale de Lyon/Université Lyon 1/INSA de Lyon,

ECL, 36 avenue Guy de Collongue, 69134 Ecully Cedex, France

[3] Department of Modern Mechanics, University of Science and Technology of China, Hefei 230027, China

Abstract. Three dimensional biglobal linear stability of Poiseuille-Rayleigh-Bénard (PRB) duct flows in binary fluids with Soret effect has been analyzed by using a two-dimensional Chebyshev collocation method in order to get the numerical dispersion relation. For a negative separation factor $\psi = -0.01$ and without throughflow, four dominant pairs of traveling tranverse modes (with finite wavenumbers k) (denoted as modes A, B, C and D) have been found and each pair corresponds to two symmetry degenerate left and right traveling modes which have the same critical Rayleigh number. With the increase of the duct aspect ratio A, the critical Rayleigh numbers for these four pairs of modes decrease and closely approach the value obtained in a two-dimensional situation, mode A always remaining the dominant mode. Oscillatory longitudinal modes (corresponding to $k = 0$) have also been found. Their critical Rayleigh numbers (above those of the transverse modes) present oscillatory variations when the aspect ratio A is increased, corresponding to longitudinal modes with an increasing number of rolls. When the pressure gradient is imposed along the duct, the induced throughflow breaks the symmetry degeneracy of the pairs of traveling transverse modes, as it was already observed in two-dimensional PRB flows. For the aspect ratio $A = 3$, the overall critical Rayleigh number in the Reynolds number range studied is determined by the upstream transverse mode A. In contrast, for larger aspect ratios as $A = 7$, different modes are successively dominant as the Reynolds number is increased, involving both upstream and downstream transverse modes A and even the longitudinal mode.

Keywords: BiGlobal instability, binary fluid, Soret effect

1. Introduction

Laminar forced and mixed convection of binary fluids in a horizontal duct heated from below has many practical technological applications like the cooling process of electronic devices and the technics of chemical vapor deposition (CVD) for the production of magnetic and optic data storage devices in the electronics industry. It also leads to a variety of spatiotemporal patterns, the study of which has a great theoretical interest. In fact, the spatiotemporal behavior of the dissipative structures appearing in binary mixture convection (Cross & Hohenberg 1993) has been revealed to be complex due to the combination of thermal forcing (characterized by the Rayleigh number Ra) and Soret coupling between temperature and concentration fields (characterized by the separation factor ψ); and the externally imposed throughflow (characterized by the Reynolds number Re) will further break the symmetries existing in the pure Rayleigh-Bénard case.

For the three-dimensional Poiseuille-Rayleigh-Bénard flow (PRB flows), most successful researches are based on the pure fluid, though for binary fluids the thresholds of the three-dimensional flows without the two extent spanwise boundaries can be deduced from the two-dimensional linear stability analysis through the Squire transformation of the full linear stability equations (Hu et al. 2007). For pure fluids, it has been revealed (Gage & Reid 1968; Luijkx et al. 1981; Platten & Legros 1984; Nicolas et al. 2000) that there exist two main unstable modes which correspond to the thermo-convective roll patterns of the transversal rolls $R_\perp$ and the longitudinal rolls $R_\parallel$. In the case of ducts of in finite lateral extension, the longitudinal rolls appear first since the critical Rayleigh number for the longitudinal rolls is always smaller than that for the transversal rolls. For finite rectangular ducts, the lateral confinement tends to stabilize both of the two modes of the basic flow. But the threshold (i.e. the critical Rayleigh number) of the longitudinal rolls which is independent of the Reynolds number and Prandtl number, increases much faster than that of the transversal rolls which increases with the increase of the Reynolds nmuber and the increase of the Prandtl number. This makes that the transversal rolls occur first at small Reynolds number while the longitudinal rolls occur first at large Reynolds number. For the convective and absolute instability study, Müller et al. (1992, 1993) have first determined the transition curve

between the convective and absolute instability zones for the transverse rolls by using a weakly non-linear theory based on a Ginzburg-Landau equation. Ouazzani et al. (1990, 1995), experimentally and Nicolas et al. (1997), numerically, have shown that the transition between the basic flow and the transversal rolls exactly corresponds to the AI/CI boundary curve, provided that the flow is not continuously perturbated near the inlet. Furthermore, for infinite extent system, by evaluating the longtime behaviour of the Green function in the horizontal plane (the concept of AI/CI refers to the papers (Briggs 1964; Bers 1973; Brevdo 1991; Huerre & Monkewitz 1985)), Carrière & Monkewitz (1999) successfully and theoretically revealed that the mode reaching zero group velocity at the convective-absolute transition always corresponds to transverse rolls, while the system remains convectively unstable with respect to pure streamwise (longitudinal) rolls for all non-zero Reynolds numbers.

So far, most researches for the three-dimensional PRB flows are based on pure fluids, the researches on binary fluids, however, focus on the two-dimensional system. With continuous advances in algorithms for the numerical solution of large nonsymmetric real/complex generalised eigenvalue problems alongside continuous computing hardware improvements, the instability of flows developing in two inhomogeneous and one homogeneous spatial direction can be analyzed (BiGlobal instability analysis). BiGlobal or TriGlobal instability analysis for all kinds of flow problems become more and more popular recent years and are reviewed by Theofilis (2003, 2011) for different applications. In this paper, linear BiGlobal stability analysis of PRB flows will be studied for binary fluids to see the difference between binary fluids with negative separation factors and pure fluids in the three-dimensional PRB flow system. The formulation of the problem is given in Sec. 2. After that, BiGlobal instabilities of PRB flows in binary fluids with negative separation factors are analyzed in Sec. 4.

2. Formulation

We consider a rectangular duct with height H (along z) and width L (along y) which is filled with a binary mixture and is heated from below (a temperature T_2 is applied at the upper wall and $T_1 > T_2$ is applied at the bottom; see the schematic representation in figure 1). A steady laminar flow may be generated inside the duct by imposing a con-stant pressure gradient along the homogeneous spatial x-direction. Due to the influence of the gravitational effect, the binary mixture may become unstable under the influence of vertical temperature and concentration gradients. To take this into account, the density variations are considered, but, according to the Boussinesq approximation, they are restricted to the buoyancy term and are expressed as a linear law,

$$\rho = \rho_0 \left[1 - \beta_T (T - T_0) - \beta_C (C - C_0)\right],$$

where β_T and β_C are the thermal and solutal expansion coefficients; ρ_0, T_0 and C_0 are reference values for density, temperature and concentration, respectively, which are taken as the mean initial values of the respective fields.

The Soret effect, which arises as the contribution of the temperature gradient to the mass flux, is considered here, whereas the Dufour effect, which arises as the contribution of the concentration gradient to the heat flux, is neglected. This assumption is valid for liquid mixtures. The mass flux J_C and the heat flux J_T are then

$$J_C = -\rho_0 D_C \nabla C - \rho_0 D_S \nabla T,$$

$$J_T = -D_T \nabla T,$$

where D_C, D_S and D_T are the solutal diffusion coeficient, Soret diffusion coeficient and thermal conductivity, respectively. The conductive steady state will then correspond to linear variations along the vertical z-direction for both the temperature and the concentration, leading to a concentration difference $\Delta C = -D_S \Delta T / D_C$ induced by the applied temperature difference $\Delta T = T_1 - T_2$.

The flow in this system is modeled by the Navier-Stokes equations coupled to an energy equation and a concentration equation. In these equations, length, velocity, time and pressure are scaled by H, κ/H, H^2/κ and $\rho_0 \kappa^2 / H^2$, respectively (κ is the thermal diffusivity). Thus the dimensionless governing equations of the three-dimensional Poiseuille-Rayleigh-Bénard flow are

$$\nabla \cdot \mathbf{v} - 0,$$

$$\frac{\partial \mathbf{v}}{\partial t} + (\mathbf{v} \cdot \nabla)\mathbf{v} = -\nabla p + Pr \nabla^2 \mathbf{v} + Ra\, Pr(\theta + \psi c)\mathbf{e}_z,$$

$$\frac{\partial \theta}{\partial t} + \mathbf{v} \cdot \nabla \theta = \nabla^2 \theta,$$

$$\frac{\partial c}{\partial t} + \mathbf{v} \cdot \nabla c = Le \left(\nabla^2 c - \nabla^2 \theta\right),$$

where v = (u, v, w) is the three-dimensional dimensionless velocity vector, $\mathbf{e}_z$ is the unit vector in the vertical direction. The dimensionless parameters appearing in the governing system are the Prandtl number Pr, the Rayleigh number Ra, the separation factor ψ, and the Lewis number Le. Ethanol-water mixtures are very convenient for studying Soret-driven flows, because the separation factor can be varied over a wide range by changing the average ethanol concentration. For typical experimental conditions, $5 < Pr < 11$ and $Le \approx 0.01$, so that $Pr = 10$ and $Le = 0.01$ are usually used to represent the values of the Prandtl number and Lewis number for ethanol-water mixtures. These are the values we will choose in our study. The separation factor ψ will be chosen as negative, a case where symmetric left and right

traveling waves are found for $Re = 0$, and its value will be fixed to $\psi = -0.01$.

The section of the rectangular duct is now defined in dimensionless units by $\Omega = y\epsilon[0, A] \times z\epsilon[0,1]$, where $A = L/H$ is the aspect ratio of the duct. The boundary conditions associated to the governing equations are then

$$\begin{aligned}
\text{no-slip conditions:} \quad & u = v = w = 0, \quad \text{at} \quad z = 0, 1 \quad \text{and} \quad y = 0, A, \\
\text{thermal conditions:} \quad & \theta = 0.5, \quad \text{at} \quad z = 0, \\
& \theta = -0.5, \quad \text{at} \quad z = 1, \\
& \partial_y \theta = 0, \quad \text{at} \quad y = 0, A, \\
\text{mass impermeability:} \quad & \partial_z \theta - \partial_z c = 0, \quad \text{at} \quad z = 0, 1, \\
& \partial_y \theta - \partial_y c = 0, \quad \text{at} \quad y = 0, A,
\end{aligned}$$

The non-dimensional basic steady state can easily be obtained by setting the linearly distributed temperature and concentration field along the bounded z-direction

$$\bar{\theta}(z) = 0.5 - z,$$

$$\bar{c}(z) = 0.5 - z,$$

and by imposing a constant pressure gradient in the unbounded x-direction with a linear profile of pressure gradient in the gravitational z-direction,

$$\nabla \bar{p} = -12Re\ Pr^2 \mathbf{e}_x + Ra\ Pr(1 + \psi)(0.5 - z)\mathbf{e}_z,$$

which drives a steady laminar flow, i.e. the Poiseuille flow. Thus the basic streamwise velocity is solved by the Poisson equation

$$\nabla_{2d}^2 \bar{u} = \frac{1}{Pr} \partial_x \bar{p} = -12Re\ Pr,$$

where $\nabla_{2d}^2 = \partial_y^2 + \partial_y^2$. The boundary conditions for the basic velocity field are

$$\bar{u}(y, z - 0) - \bar{u}(y, z - 1) - \bar{u}(y - 0, z) - \bar{u}(y - A, z) - 0.$$

The disturbed three-dimensional Poiseuille-Rayleigh-Bénard flow with Soret effect can be decomposed as

$$u = \bar{u} + u',\ v = v',\ w = w',\ p = \bar{p} + p',\ \theta = \bar{\theta} + \theta' \text{ and } c = \bar{c} + c',$$

where the primes refer to small perturbation quantities. After substituting these variables into the governing equations and neglecting the terms which are quadratic with respect to the perturbations, we can obtain the linearized perturbation equations (for brevity not presented here). The perturbation quantities can further be expanded as normal modes,

$$(u', v', w', p', \theta', c') = [\hat{u}(y, z), \hat{v}(y, z), \hat{w}(y, z), \hat{p}(y, z), \hat{\theta}(y, z), \hat{c}(y, z)] \exp[i(kx - \omega t)],$$

where k is a real wavenumber and ω a complex frequency. Substituting these expressions in the linearized system, we obtain the linear stability equations expressed as

$$ik\hat{u} + D_y\hat{v} + D_z\hat{w} = 0,$$

$$-i\omega\hat{u} + ik\bar{u}\hat{u} + (D_y\bar{u})\hat{v} + (D_z\bar{u})\hat{w} = -ik\hat{p} + Pr(D^2 - k^2)\hat{u},$$

$$-i\omega\hat{v} + ik\bar{u}\hat{v} = -D_y\hat{p} + Pr(D^2 - k^2)\hat{v},$$

$$-i\omega\hat{w} + ik\bar{u}\hat{w} = -D_z\hat{p} + Pr(D^2 - k^2)\hat{w} + Ra\ Pr(\hat{\theta} + \psi\hat{c}),$$

$$-i\omega\hat{\theta} + ik\bar{u}\hat{\theta} + (D_z\bar{\theta})\hat{w} = (D^2 - k^2)\hat{\theta},$$

$$-i\omega\hat{\eta} + ik\bar{u}\hat{\eta} = (D^2 - k^2)\hat{\theta} + Le(D^2 - k^2)\hat{\eta},$$

where

$$\eta = \theta - c,\ D_y = \partial_y,\ D_z = \partial_z \text{ and } D^2 = \partial_y^2 + \partial_z^2.$$

The corresponding boundary conditions are

$$\begin{aligned}
\text{no-slip conditions:} \quad & \hat{u} = \hat{v} = \hat{w} = 0, \quad \text{at} \quad z = 0, 1 \quad \text{and} \quad y = 0, A, \\
\text{thermal conditions:} \quad & \hat{\theta} = 0, \quad \text{at} \quad z = 0, 1, \\
& D_y\hat{\theta} = 0, \quad \text{at} \quad y = 0, A, \\
\text{mass impermeability:} \quad & D_z\hat{\eta} = 0, \quad \text{at} \quad z = 0, 1, \\
& D_y\hat{\eta} = 0, \quad \text{at} \quad y = 0, A.
\end{aligned}$$

The linear stability equations are two-dimensional partial differential equations, and if there exists a nontrivial solution for the equations, a corresponding dispersion relation

$$D(k, \omega; Ra, Re, \psi, Pr, Le) = 0$$

should be satisfied, and we need to solve a biglobal eigenvalue problem. Because it is impossible to find the explicit analytical dispersion relation if there is no further simplification, the dispersion relation has to be obtained numerically.

In this paper, the two-dimensional Chebyshev spectral collocation method (Canuto et al. 2006) is used to discretize the eigenvalue problem and the implicitly restarted Arnoldi method (Lehoucq & Sorensen 1996) to solve the resulting general eigenvalue problem.

3. BiGlobal instability analysis

The pure Rayleigh-Bénard situation for binary fluids (Pr = 10, Le = 0.01, $\psi = -0.01$) in a duct without throughflow is first considered by setting Re = 0. In such a case with negative Soret effect and for A = 5 and Ra = 2000, four unstable oscillatory modes, corresponding to symmetry degenerate left and right traveling modes and labelled as A, B, C and D, are found for k = 3.14. The convergence of the four corresponding eigenvalues with the grid size is shown in Table 1. We see that the least stable modes have fastest convergence, and that for the mode D with the slowest convergence, there is already have valid digits in the eigenvalue for the 32 × 32 resolution. Such a 32 × 32 grid has been used for most computations in this paper.

The neutral curves for these four modes, plotted in the parameter plane k - Ra, are given in figure 2 for different duct aspect ratios A. We see that with the increase of the aspect ratio, the four neutral curves for these modes become closer and the parts of these curves corresponding to longitudinal modes (weak k values) eventually disappear from the graph (they could, however, exist for larger Ra values). This seems to indicate that the four curves would merge to give a single neutral curve for $A \to \infty$, i.e. in the two-dimensional limiting case. In fact, for the corresponding two-dimensional Rayleigh-Bénard situation with Soret effect (Pr = 10, Le = 0.01 and $\psi = -0.01$), the critical Rayleigh number is Ra_c = 1743.894, and the critical wavenumber is k_c = 3.117. The different curves seem to all evolve towards these critical values as A is increased. The curve of mode A, however, evolves more quickly and this curve is already quite close to the two-dimensional critical values for A = 5.

The spatial structure of these modes is shown in figure 3 through their temperature distributions at their critical values for a large aspect ratio, A = 10 (these structures are taken at a fixed time). These spatial structures are obtained from the eigenvectors at threshold. If the discretized eigenvector is denoted as $X = X_r + iX_i$, the perturbation for k and ω_r non equal to zero will be given by $\Re\left(Xe^{i(kx-\omega_r t)}\right) = X_r \cos(kx - \omega_r t) - X_i \sin(kx - \omega_r t)$, where $\Re$ denotes the real part. We see that the four modes shown in figure 4 are clearly different as they have different spatial structures in the cross-section. More precisely, modes A, B, C and D have two, three, four and five roll structures in the cross-section, respectively.

We now investigate the throughflow effect on the critical Rayleigh number for the different dominant modes. The critical curves for the first four unstable oscillatory transverse modes as a function of the Reynolds number Re are first given for small Re and A = 5 in figure 4. We recall that for Re = 0 these oscillatory transverse modes correspond to symmetry degenerate left and right traveling modes. This symmetry is broken by the throughflow, which will differently infuence the thresholds of the left and right traveling modes, which, in the following, will rather be presented as upstream and downstream modes, respectively.

The results presented in figure 4 have been obtained for modes traveling in the positive x direction and for throughflows either in the positive (Re > 0) or negative (Re < 0) x direction. If we now refer to the direction of the throughflow, the results obtained for Re > 0 (Re < 0) will be those associated with the effect of the throughflow on the downstream (upstream) modes. When the transverse modes A, B, C and D are considered as downstream modes (Re > 0), the increase of the throughflow from Re = 0 induces a continuous increase of their critical Rayleigh numbers. In contrast, when they correspond to upstream modes (Re < 0), with the increase of the throughflow from Re = 0 (increase of $|\mathrm{Re}|$ the critical thresholds first decrease, reach a minimum value and then increase more quickly. Note that the critical values associated with the transverse mode A remain the smallest in the Re range studied here, indicating that this mode A is the dominant transverse mode. Concerning the longitudinal modes (k = 0), they are not influenced by the throughflow, so that their critical thresholds do not depend on Re.

To better see the selective influence of the throughflow on the instabilities, we now compare the critical thresholds obtained for the different dominant modes, i.e. the downstream and upstream transverse A modes and the dominant longitudinal mode (estimated for k = 0.01). The critical curves for these three modes are plotted as a function of Re (Re > 0) for three values of the aspect ratio A (A = 3, 5 and 7) in figure 5. For A = 3 (figure 5(a)), the critical curve for the upstream transverse mode is below that for the downstream transverse mode and also below the critical value for the longitudinal mode ($Ra_c \approx$ 1916.6, slightly outside the Ra_c range considered in the figure). For A = 3, the upstream transverse mode is then the dominant mode and its critical curve is the true critical curve within the Re range studied ($Re \leq$ 0.45).

For A = 5 (figure 5(b)), the dominant mode in the Re range studied is still the upstream transverse mode. However, the critical curve for the downstream transverse mode is now almost in contact with the critical curve for the upstream transverse mode for Reynolds numbers in the range 0.1 ≤ Re ≤ 0.16. Moreover, the horizontal line corresponding to the critical value for the longitudinal mode ($Ra_c \approx$ 1821.35) intersects the critical curve for the downstream transverse mode at Re = 0.258, indicating that beyond this value, the longitudinal mode is more dangerous than the downstream transverse mode.

Finally, for A = 7 (figure 5(c)), due to different intersections between the critical curves, the dominant mode will depend on the value of Re. For small values of Re ($0 \leq Re \leq 0.09$), the dominant mode is still the upstream transverse mode. In the range $0.1 \leq Re \leq$ 0.19, because of the crossings between the transverse mode curves, the downstream transverse mode becomes the dominant mode. The upstream transverse mode is again the dominant mode in a small

range $0.2 \leq Re \leq 0.22$. Finally, for the larger values of Re considered in the graph ($0.23 \leq Re \leq 0.4$), the longitudinal mode becomes the dominant mode because its critical threshold $Ra_c \approx 1790.01$ is now below the thresholds for the two transverse modes.We can expect to find such changes of modes when Re is increased for larger values of A. The Re ranges associated to the different modes, however, will change because of the decrease of the longitudinal mode critical value and the more important crossings between the transverse mode critical curves.

4. References

[1] Bers, A. 1973 Theory of absolute and convective instabilities. In *International Congress on Waves and Instabilities in Plasma* (ed. G. Auer & F. Cap), pp. B1-B52. Innsbruck, Austria.

[2] Brevdo, L. 1991 Three-dimensional absolute and convective instabilities, and spatially amplifying waves in parallel shear flows. *Z. Angew. Math. Phys*. 42, 911-942.

[3] Briggs, R. J. 1964 Electron-Stream Interaction with Plasmas. MIT Press.

[4] Canuto, C., Hussaini, M. Y., Quarteroni, A. & Zang, T.A. 2006 *Spectral Methods: Fundamentals in Single Domains*. Berlin: Springer.

[5] Carrière, Ph. & Monkewitz, P. A. 1999 Convective versus absolute instability in mixed rayleigh-bénard-poiseuille convection. *J. Fluid Mech*. 384, 243-262.

[6] Cross, M. C. & Hohenberg, P. C. 1993 Pattern formation outside of equilibrium. *Rev. Mod. Phys*. 65, 851.

[7] Gage, K. S. & Reid, W. H. 1968 The stability of thermally stratified plane poiseuille flow. *J. Fluid Mech.* 33, 21-32.

[8] Hu, J., Ben Hadid, H. & Henry, D. 2007 Linear stability analysis of Poiseuille-Rayleigh-Bénard flows in binary fluids with Soret effect. *Phys Fluids* 19, 034101.

[9] Huerre, P. & Monkewitz, P. A. 1985 Absolute and convective instabilities in free shear layers. *J. Fluid Mech*. 159, 151.

[10] Kato, Y. & Fujimura, K. 2000 Prediction of pattern selection due to an interaction between longitudinal rolls and transverse modes in a flow through a rectangular channel heated from below. *Phys. Rev. E* 62, 601-611.

[11] Lehoucq, R. B. & Sorensen, D. C. 1996 Deflation Techniques for an Implicitly Restarted Arnoldi Iteration. SIAM.

[12] Luijkx, J. M., Platten, J. K. & Legros, J. C. 1981 On the existence of thermoconvective rolls, transverse to a superimposed mean poiseuille flow. *Intl J. Heat Mass Transfer* 24, 1287-1291.

[13] Müller, H. W., Lücke, M. & Kamps, M. 1992 Transversal convection patterns in horizontal shear flow. *Phys. Rev.* A 45, 3714-3726.

[14] Müller, H. W., Tveitereid, M. & Trainoff, S. 1993 Rayleigh-bénard problem with imposed weak through-flow: Two coupled ginzburg-landau equations. *Phys. Rev*. E 48, 263-272.

[15] Nicolas, X., Luijkx, J. M. & Platten, J. K. 2000 Linear stability of mixed convection flows in horizontal rectangular channels of finite transversal extension heated from below. *International Journal of Heat and Mass Transfer* 43, 589-610.

[16] Nicolas, X., Mojtabi, A. & Platten, J. K. 1997 Two-dimensional numerical analysis of the poiseuille-benard flow in a rectangular channel heated from below. *Phys. Fluids* 9, 337-348.

[17] Ouazzani, M. T., Platten, J. K. & Mojtabi, A. 1990 Etude numérique et expérimentale de la convection mixte entre deux plans horizontaux à températures différentes ii. *Intl J. Heat Mass Transfer* 33, 1417-1427.

[18] Ouazzani, M. T., Platten, J.-K., Müller, H. W. & Lücke, M. 1995 Etude de la convection mixte entre deux plans horizon-taux à des températures différentes - iii. *Int. J Heat Mass Transfer* 38, 875-886.

[19] Platten, J.-K. & Legros, J.-C. 1984 *Convection in Liquids.* Springer Verlag, Berlin, Heidelberg.

[20] Theofilis, V. 2003 Advances in global linear instability analysis of nonparallel and three-dimensional flows. *Prog. Aero. Sci*. 39, 249-315.

[21] Theofilis, V. 2011 Global linear instability. *Annu. Rev. Fluid Mech.* 43, 319-352.

Resolution	mode A	mode B
24×24	$\pm 1.4332535922 + 1.3844131577i$	$\pm 1.7006743356 + 1.2496657103i$
28×28	$\pm 1.4332537142 + 1.3844131715i$	$\pm 1.7006746271 + 1.2496655484i$
32×32	$\pm 1.4332537421 + 1.3844131747i$	$\pm 1.7006746820 + 1.2496655193i$
36×36	$\pm 1.4332537504 + 1.3844131762i$	$\pm 1.7006746989 + 1.2496655130i$
40×40	$\pm 1.4332537534 + 1.3844131767i$	$\pm 1.7006747054 + 1.2496655106i$
Resolution	mode C	mode D
24×24	$\pm 2.1119229402 + 0.8249930660i$	$\pm 2.4525308870 + 0.0436264770i$
28×28	$\pm 2.1119248269 + 0.8249915138i$	$\pm 2.4525304703 + 0.0436271347i$
32×32	$\pm 2.1119253499 + 0.8249911402i$	$\pm 2.4525309750 + 0.0436268660i$
36×36	$\pm 2.1119255169 + 0.8249910206i$	$\pm 2.4525310423 + 0.0436267111i$
40×40	$\pm 2.1119255771 + 0.8249909772i$	$\pm 2.4525310608 + 0.0436266659i$

TABLE 1. Tests of accuracy for the eigenvalues corresponding to the first four unstable oscillatory modes found for $k = 3.14$, $A = 5$, $Ra = 2000$, $Re = 0$, $Pr = 10$, $Le = 0.01$ and $\psi = -0.01$.

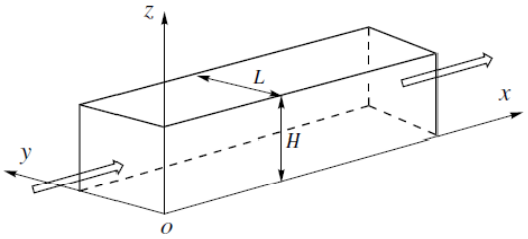

Fig1. Schematic representation of the Poiseuille-Rayleigh-Bénard (PRB) duct flows.

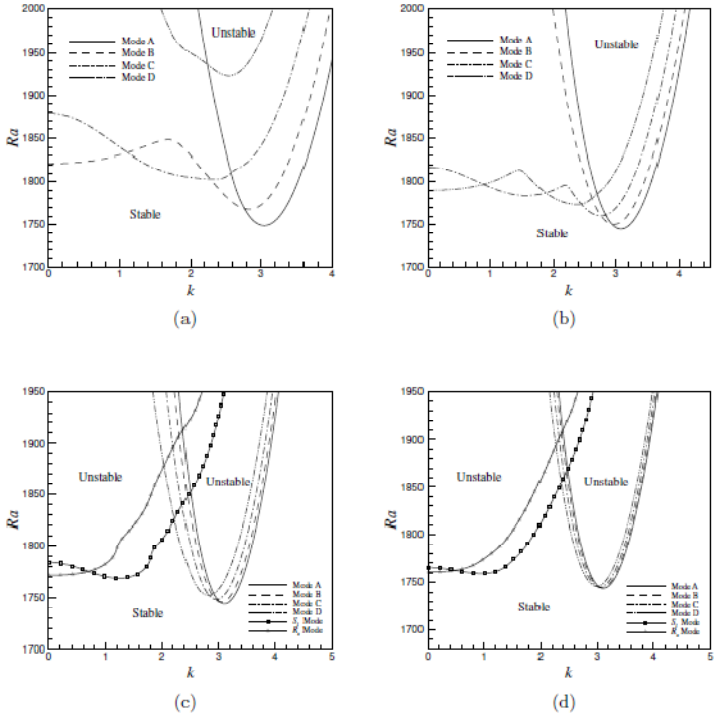

Fig 2. Neutral curves for the first four unstable oscillatory modes in the parameter plane *k*-*Ra* for (a) *A*=5, (b) *A*=7, (c) *A*=10 and (d) *A*=15.

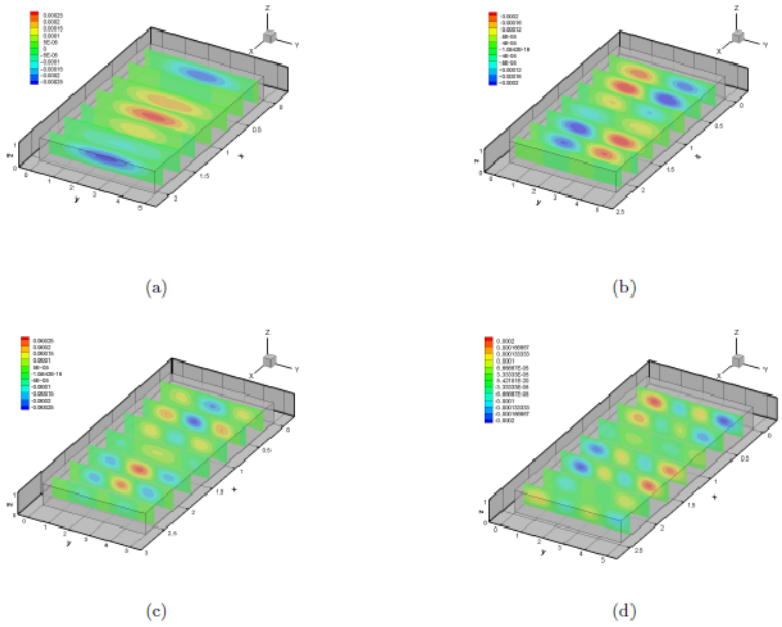

Fig 3. Temperature eigenstructure for the first four unstable traveling transverse modes at their critical points for $A = 10$: (a) $Ra = 1744.38$, $k = 3.100$, $\omega_r = 1.932$ (mode A), (b) $Ra = 1745.90$, $k = 3.048$, $\omega_r = 1.935$ (mode B), (c) $Ra = 1748.55$, $k = 2.957$, $\omega_r = 1.940$ (mode C), (d) $Ra = 1752.50$, $k = 2.817$, $\omega_r = 1.943$ (mode D).

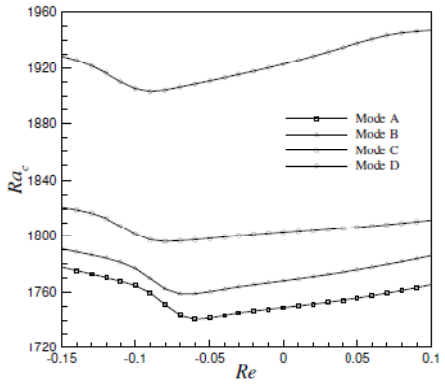

Fig 4. Critical curves for the first four unstable traveling transverse modes as a function of the Reynolds number Re when $A = 5$.

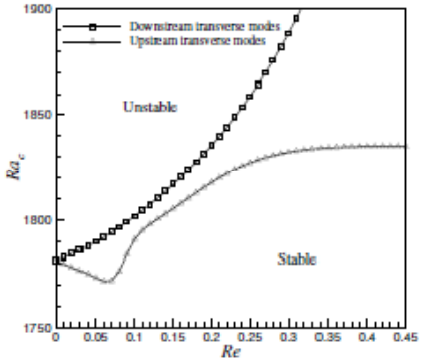

(a)

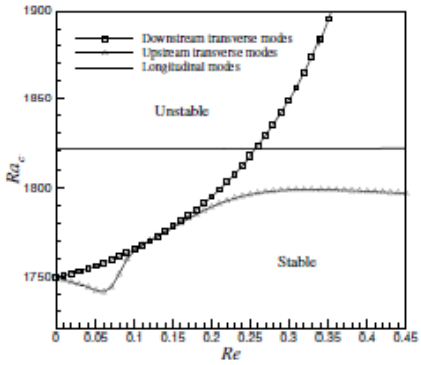

(b)

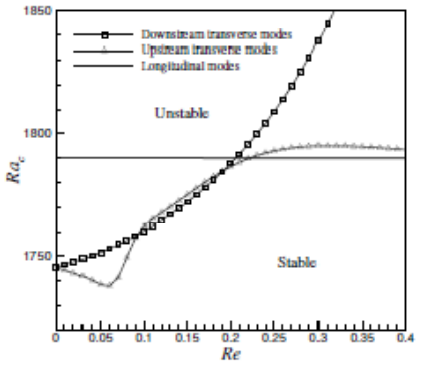

(c)

Fig 5. Critical curves for the dominant upstream and downstream transverse modes and the dominant longitudinal mode (k = 0.01) as a function of the Reynolds number Re: (a) A = 3, (b) A = 5 and (c) A = 7.